

# ELECTRON COOLING EXPERIMENT AT HIMAC SYNCHROTRON

K. Noda, T. Furukawa, S. Shibuya, M. Muramatsu, T. Honma, E. Takada, S. Yamada, NIRS, Japan  
 E. Syresin, JINR, Dubna, Moscow region, Russia  
 H. Ogawa, T. Iwashima, A. Takubo, AEC, Chiba, Japan  
 H. Uchiyama, D. Tann, Chiba University, Chiba, Japan  
 T. Nagafuchi, K. Maeda, Toshiba, Tokyo, Japan  
 H. Fadil, T. Shirai, A. Noda, ICR, Kyoto University, Uji, Japan

## Abstract

Electron-cooling experiments have been being carried out at HIMAC in order to provide high-quality and high-intensity beam for medical and other applications. The paper reports the results of the cooling experiment and the simulation.

## 1 INTRODUCTION

The HIMAC (Heavy Ion Medical Accelerator in Chiba) accelerator complex has delivered  $^{12}\text{C}$  beams for the cancer therapy and other heavy-ions for basic and applied research [1]. One of the objectives of HIMAC is to develop new technologies in heavy-ion therapy and related basic and applied research. For the purpose, it is very important to improve beam property and enhance capability of handling it. The electron-cooling method can provide high-intensity or high-quality beams by cool stacking and by its strong phase-space compression. The aim of our study is to apply those techniques of accelerator physics to medical and other fields. These techniques will lead to the following:

- (1) An increase in the intensities of heavier ions, such as Fe and Ni, for estimation of radiation risk in space.
- (2) Micro-beam probe for the cellular radiation-response.
- (3) Short bunched beam for time-resolving measurements.

Thus an electron cooler was constructed [2] and installed to the HIMAC synchrotron, and cooling experiments have been carried out [3]. The paper reports the experimental results and the comparison with the simulation described in detail in the ref. [4].

## 2 EXPERIMENTAL CONDITIONS

Fully stripped argon-ions with the energy of 6.0 MeV/n have been used in the cooling experiments. In order to observe cooling phenomena easily, the horizontal emittance is decreased to around 65 from 264  $\pi$ -mm-mrad by decreasing the time-width of the injection beam, while the vertical one is kept around 10  $\pi$ -mm-mrad. A revolution frequency of circulating ions was measured by observing higher-harmonics of Schottky signal in order to determine electron energy. The electron energy was

determined precisely by changing the energy so as to maximise a bunch signal in applying RF field with amplitude of  $\pm 10\text{V}$ . The bucket height corresponding to the RF amplitude is almost consistent with a linear regime that is proportional to a gradient of a velocity profile. An MCP monitor, having a spatial resolution of 0.3 mm at  $\sigma$ , non-destructively measured beam profiles in both the horizontal and vertical planes [5]. The experimental conditions are summarised at Table 1.

Table 1. The conditions of the cooling experiment

Electron energy ( $T_e$ )	3.465 keV
Electron current ( $I_e$ )	0.1 – 0.2 A
Expansion factor ( $R_{\text{EXP}}$ )	3.3
Electron-beam diameter	64 mm
Field strength at gun section	0.167T
Field strength at cooling section	0.05 T
-----	
Argon-ion energy	6.00 MeV/n
Initial momentum spread	$1 \cdot 10^{-3}$ at FWHM
Tune ( $Q_x/Q_y$ )	3.68/2.88
$\beta_x/\beta_y$ in cooling section	9.9m/10.7m
Dispersion in cooling section $D_x$	2.2 m
Transition energy, $\gamma_t$	3.7
Phase slip factor, $\eta$	0.93

## 3 COOLING EXPERIMENTS

### 3.1 Dependence of beam alignment on cooling

In order to investigate the dependence of the beam alignment on the transverse cooling, the beam size after cooling of 2 s was measured by the MCP monitor, as a function of the angle of the electron-beam axis [6]. Figure 1 shows the measurement and simulation results. It is noted that the ion-beam size before the cooling was around 30 mm at FWHM. The simulation was carried out, further, under the conditions of an electron current ( $I_e$ ) of 0.2 A, a transverse electron temperature of 30 meV and a longitudinal one of 0.07 meV. The simulation result in a small misalignment angle is consistent with the measurement one, while that in a large angle region is

quite difference. In addition, the electron-beam offset did not strongly affect the cooling, compared with the angle.

The beam profiles in both the horizontal and vertical planes were measured as a function of cooling time just after multiturn injection. In the  $I_c$  of 0.2 A, the horizontal beam size was in equilibrium at 1.3 mm (FWHM) after 3 s cooling. As shown in Fig. 2, it seems that it was slightly fast for the vertical beam size to be reached in equilibrium, compared with the horizontal one, while that in the  $I_c$  of 0.1 A was more than 4 s. Figure 2 shows also the simulation results under the misalignment angle ( $\alpha$ ) of 0.9 mrad, which are in agreement with the measurement one in both the  $I_c$  of 0.1 and of 0.2 A. Thus the misalignment between the electron and ion axes is estimated to be around 1 mrad.

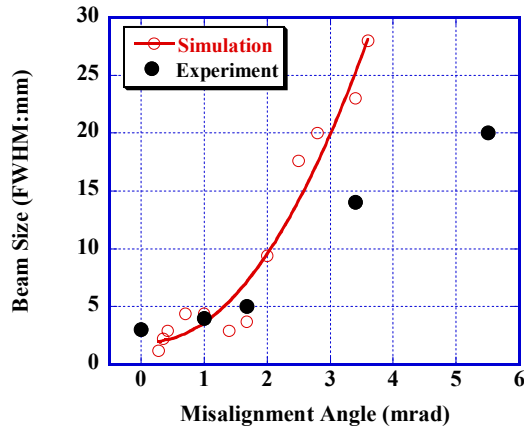


Fig. 1: Dependence of beam alignment on horizontal cooling. Closed and open circles indicate the measurement and simulation results, respectively. The solid line is an eye-fit of the simulation result.

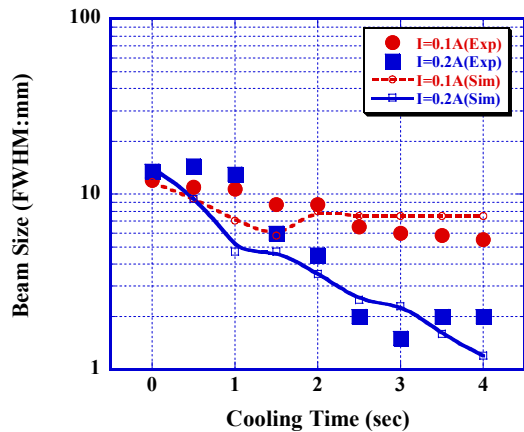


Fig. 2: Cooling-time measurement. Closed circles and squares indicate the vertical beam size as a function of cooling time in the  $I_c$  of 0.1 and 0.2 A, respectively. The broken and solid lines are the simulation results in the  $I_c$  of 0.1 and 0.2 A, respectively.

### 3.2 Intra-beam scattering (IBS)

The balance between an electron cooling and an IBS heating determines the equilibrium beam size. Thus we measured the beam-size growth after switching the electron cooling off. Figure 3 shows the measurement results. According to the analysis [7], the beam-size growth is given by

$$\sigma(t) = (\gamma D_0 t + \sigma_0^\gamma)^{1/\gamma} \quad (1),$$

where  $D_0$  is a constant being proportional to  $(Z^2/A)^2 N$ :  $Z$ ,  $A$  and  $N$  are a charge state, mass number and number of ions, respectively. Fitting these data to equation (1),  $\gamma$  is estimated to be  $6.0 \pm 0.7$ . As shown in Fig. 3, the simulation result under the  $\gamma$  of 7 and the  $N$  of  $2 \cdot 10^6$  is consistent with the measurement one, while the analysis expects to be the  $\gamma$  of 5. In this simulation,  $\lambda$  is estimated to be around  $1 \text{ s}^{-1}$  in the initial beam size.

The horizontal beam-size in equilibrium was measured as a function of the beam intensity. Figure 4 shows the experiment and the simulation results. The simulation is carried out under transverse electron temperatures of 100, 50 and 30 meV. It is noted that this simulation does not take into account the misalignment effect. It is observed from the figure that the experiment result is fairly consistent with the simulation one under the electron temperature of 50 meV rather than other temperatures. This temperature is larger than 30 meV estimated under an expansion factor of 3.3 and a cathode temperature of 100 meV. The difference corresponds to the  $\alpha$  of 1 mrad, which supports the result described at the section 3.1.

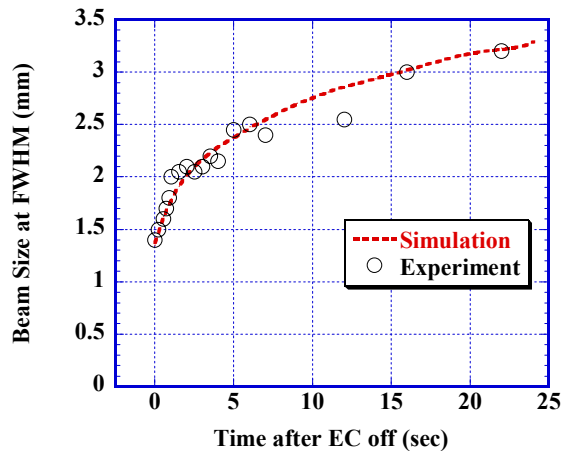


Fig. 3: IBS heating measurement. Open circles indicate the beam-size as a function of the time after switching the cooling off. The broken line indicates the simulation result.

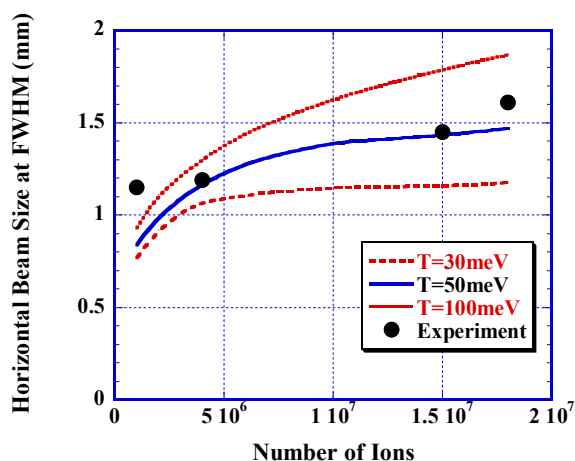


Fig. 4: The equilibrium beam size as a function of the beam intensity. Closed circles indicate the measurement result. Broken, solid and dotted lines indicate the simulation results under the transverse electron temperature of 100, 50 and 30 meV, respectively.

### 3.3 Cool stacking and instability

The cool stacking increases beam intensity. The beam was injected to the ring in a period of 3.3 sec by the multiturn-injection method. The intensity gain by the cool stacking was around 10, which depends on a cooling rate and a beam lifetime. As increasing the intensity, a vertical coherent oscillation, having the frequency corresponding to the bare tune, was observed, and the amplitude was increasing by twice during around 0.2 s. This instability suggests the possibility of the electron-heating effect [8].

### 3.4 Short-bunched beam

The cooling and applying RF field can obtain a short-bunched beam. A saw-tooth-wave of the RF field is suitable for production of a short bunched beam compared with a sinusoidal one, because of no filamentation. A short-bunched beam with around 50 ns at FWHM was obtained in using the saw-tooth-wave RF field and the cooling, while that with 80 ns in the sinusoidal RF field. As figure 5 shows the RF voltage dependency of the bunch width, the bunch width is linearly decreasing with increasing the RF voltage. In the beam-intensity higher than around  $10^8$  ppp, as cooling the ion beam down with the RF field, several peaks were observed in one bunch, and the bunch width was considerably widened to around 400 ns at FWHM. At the same time, the transverse instability was observed as similar as that in the cool stacking.

### 3.5 Acceleration and extraction of cooled beam

After cooling for the flat base of 1 s, the cooled beam was accelerated to 50 MeV/n from the injection energy. As a result of the profile measurement in just after the acceleration, the horizontal and vertical rms-emittance are

reduced to 1.1 and  $0.4\pi$  mm-mrad from 15.7 and  $2.2\pi$  mm-mrad, respectively. After the normal injection and acceleration to 50 MeV/n, further, the beam was slowly extracted during around 2 s through the RF-KO method, along with cooling down at the flat top. The extracted-beam size was reduced to half in the vertical plane, compared with that without cooling. The reduction of the beam size through the cooling is relatively small compared with that in 6 MeV/n, because the cooling time is proportional to  $\beta^3\gamma^5$ . The horizontal size was not change, on the other hand, because it is determined by the turn-separation in the resonant-extraction process.

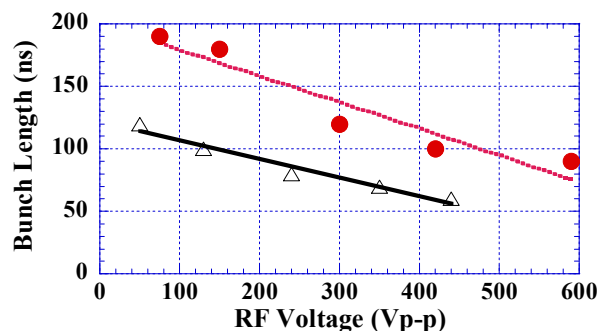


Fig. 5: The RF voltage dependency of the bunch width. Circles and triangles indicate bunch width in the sinusoidal RF and in saw-tooth-wave one, respectively.

## ACKNOWLEDGEMENT

The authors would like to express their thanks to the colleague of Accelerator Physics and Engineering Department of NIRS for continuous encouragement, and the crew of AEC for skilful operation of HIMAC.

## REFERENCES

- [1] E. Takada *et al.*, "Present Status of HIMAC", Proc. 13<sup>th</sup> SAST, Osaka, 2001, pp.187-189.
- [2] K. Noda, *et al.*, "Electron cooler for medical and other application at HIMAC", Nucl. Instrum. Meth. **A441** (2000) 159-166.
- [3] K. Noda *et al.*, "Commissioning of Electron Cooler for Medical and Other Application at HIMAC", Proc. 7<sup>th</sup> EPAC, Vienna, 2000, p.1259-1261.
- [4] E. Syresin, K. Noda and S. Shibuya, "Electron cooling in HIMAC", 14<sup>th</sup> Int'l Symposium on Heavy Ion Inertial Fusion, Moscow.
- [5] T. Honma *et al.*, "Design and Performance of A Non-destructive Beam-Profile Monitor Utilizing Charge-division Method at HIMAC", to be published in Nucl Instrum. Meth. A.
- [6] T. Furukawa *et al.*, "Beam Alignment for Electron Cooling at HIMAC", Proc. 13<sup>th</sup> SAST, Osaka, 2001, pp.384-386.
- [7] M. Beutlespacher *et al.*, "Longitudinal and transverse electron cooling experiments at Heidelberg heavy-ion storage ring TSR", Nucl. Instrum. Meth. **A441** (2000) 110-115.
- [8] V. V. Parhomchuk, "Recent development in electron cooling and its applications", Proc. APAC'98, Tsukuba, 1998, pp.462-464.